

Hidden mechanical oscillatory state in a carbon nanotube revealed by noise

P. Belardinelli,¹ W. Yang,² A. Bachtold,² M.I. Dykman,³ and F. Alijani^{4,*}

¹*Department of Construction, Civil Engineering and Architecture,
Polytechnic University of Marche, Ancona, Italy*

²*ICFO - Institut de Ciències Fotoniques, The Barcelona Institute
of Science and Technology, 08860 Castelldefels, Barcelona, Spain*

³*Department of Physics and Astronomy, Michigan State University, East Lansing, MI 48824, USA*

⁴*Department of Precision and Microsystems Engineering,
Delft University of Technology, Mekelweg 2, 2628CD, Delft*

Carbon nanotubes are devices of choice for investigating the interplay between electronic transport and nanomechanical motion. In this work, we report the co-existence of thermal vibrations and large-amplitude self-sustained oscillations in a carbon nanotube that originates from electron tunneling and thermal effects. The measured transitions between the two states are described by a Poisson process, revealing that the interstate switching is induced by noise. We observe the coexistence of the stable low-amplitude thermal state and the stable large-amplitude state (limit cycle) over a finite parameter range, which points to an isola bifurcation. We propose a minimalistic model based on nonlinear friction to account for the isola. Our work provides evidence for a new type of bifurcation leading to self-sustained oscillations that largely differs from the classical Hopf bifurcation, since these large-amplitude oscillations are a hidden state that can be unveiled via stochastic switching. We envision that this new dynamical regime and the means to reveal it will be of interest for various mesoscopic vibrational systems.

Introduction

Nano-electro-mechanical systems (NEMS) provide a means for studying physics away from thermal equilibrium in a well-characterized setting [1]. An important group of non-equilibrium phenomena originates from the interplay between nonlinearity and fluctuations in driven systems, which can modify the frequency stability [2–4], the power spectrum [5, 6], and can lead to thermal noise squeezing [6–8]. The interplay is most nontrivial when the system is brought into a regime where it has coexisting stable states. Here, fluctuations, even if weak on average, can cause interstate transitions and are ultimately responsible for the distribution of a system over the stable states. Much work on studying these effects and the emerging scaling [9, 10] has been carried out on nano- and micromechanical resonators driven by an external force or modulated parametrically [5, 11–17]. Vibration bistability and interstate switching were also predicted to emerge at a constant potential bias in the Coulomb blockade regime where single-electron tunneling to a NEMS is strongly coupled to a fluctuating nanomechanical mode in the absence of periodic driving [18]. Coexistence of stable states of a fluctuating nanomechanical mode in a different regime, also without periodic driving, was observed in a biased carbon nanotube (CNT) [19], and the onset of bistability in the regime of [18] was reported in Ref.[20].

In almost all NEMS studied thus far the vibrations could be brought to one of the stable states by smoothly changing a control parameter, for example, the driving force. As a result of the change, at some critical parameter value, bifurcation point, one of the stable states

would lose stability and the system would switch to another stable state. In the vicinity of the bifurcation point and close to the fading state the system is “soft”, as near a phase transition, making it particularly sensitive to classical and quantum fluctuations. However, fluctuations are not needed to observe the bifurcation and the onset of a new stable state.

In this paper we study the interstate switching in a qualitatively different setting. The switching occurs in a carbon nanotube between small-amplitude thermal vibrations about the quiet state and large-amplitude self-sustained oscillations. The statistical analysis that we develop allows us to identify transitions between these two states and to show that they are described by a Poisson process, indicating independent uncorrelated events. These data are consistent with a scenario, where the vibration bistability is actually *revealed* by fluctuations. The new large-amplitude stable vibrational state still emerges where the control parameter crosses a bifurcation point, but the initially occupied quiet state does not lose stability and the emerging large-amplitude state is well separated from it in phase space. Moreover, as the parameter is further changed, the large-amplitude state is observed to lose stability itself. Therefore, the self-sustained oscillatory state is made visible thanks to the presence of fluctuations – the fluctuations result in random switching into this state. Interestingly, there is no hysteresis when the bifurcation parameter is moved back and forth. In terms of the bifurcation theory, the emerging and disappearing stable state is associated with an “isola”, an isolated closed curve of the branches of the solutions of noise-free equations of motion [21].

To support our findings, we also develop a minimalistic model that describes the onset of an isolated branch. The model and the underlying physics of the self-sustained vi-

* Corresponding author (f.aliyani@tudelft.nl).

brations, including the way they are excited, are qualitatively different from the physics of the onset of an isolated branch of the response to a resonant drive found earlier [22] for a two-mode micromechanical system.

Results

Measurements. Clamped-clamped CNTs are grown by chemical vapour deposition across two metallic contact electrodes [23]. The measurements are then performed at cryogenic temperature (70mK) by applying a voltage bias to the source (S) electrode (V_{sd}) and to the gate (G) electrode (V_g) which is placed at the bottom of the CNT. The current from the drain (D) electrode is measured by using a RLC resonant circuit with $f_{RLC}=1.27$ MHz and a low-temperature HEMT amplifier (Fig. 1 a). The read-out signal is obtained by measuring the current noise spectrum δI , which is converted to the nanotube displacement at the vibration antinode δz as $\delta I = \beta \delta z$, where β is the calibration factor that depends on the transconductance of the nanotube (for details see Methods section of [19]). The same β is used to convert the lock-in measurements, from which we obtain δI directly (with two components δI_X and δI_Y), into the quadratures of the motion by $X = \delta I_X/\beta$, and $Y = \delta I_Y/\beta$. The scaled vibration amplitude is thus $R = \sqrt{X^2 + Y^2}$.

When sweeping up the source-drain voltage V_{sd} at $V_g = -616$ mV, we observe a sudden jump up in the displacement R for $V_{sd} \approx 0.2$ mV followed by a jump down at $V_{sd} \approx 0.4$ mV (Fig. 1 b). We analyse the dynamics in the phase-space of the two quadratures of motion at $V_{sd} = 0.35$ mV in Fig. 1 c. In the (X,Y) space we recognize a doughnut-like trajectory with a nonzero mean amplitude that encircles the thermal motion about the origin of the quadrature space, suggesting the onset of an oscillatory state. This new dynamical state is observed in the region $V_{sd} \in [0.2, 0.4]$ mV (highlighted in Fig. 1 b).

Importantly, we note that the change of δz^2 with V_{sd} does not resemble that of a vibrational system undergoing classical Hopf bifurcation, characterized by a smooth monotonic increment of the oscillation amplitude [24]. Interestingly, when tracing the motion amplitude as a function of time, we noticed intermittent dynamics with no periodicity (see Fig. 1 d). However, when plotting the normalized histogram of the motion amplitude R , we notice the presence of two peaks, suggestion that the system has two different dynamical states (see Fig. 1 e). It is thus important to characterize our observation and distinguish if it the dynamics is of stochastic or deterministic nature.

Co-existence of Brownian dynamics and self-sustained oscillations. To better understand the intermittent dynamics, we perform statistical analysis on the time-domain data showed in Fig. 1 d. We begin by assuming that our system has two stable states, namely a zero-amplitude state and a self-sustained oscillatory state with a large amplitude compared to the root-mean-square amplitude fluctuations. We then investigate

whether noise can induce stochastic transitions between these two states, in a scenario analogous to the noise-induced hopping of a damped particle in a double-well potential, separated by a hill-top unstable equilibrium, as sketched in Fig. 2 a. The difference, though, is that, unlike the stochastic motion in a double-well potential where the potential minimum in each well represents a static equilibrium state, here one of the stable states is a static equilibrium point, which is indeed a minimum of the potential of the nanotube, whereas the other is an out-of-equilibrium vibrational state.

The analysis of noise-induced switching in continuous dynamical systems is simpler when the switching rate is much smaller than the relaxation rate. A noise-driven system then spends most of the time fluctuating about one or the other of its stable states. The characteristic correlation time t_r of these fluctuations is the dynamical relaxation time (or the correlation time of the noise, which we assume to be shorter than t_r). Occasionally there occur large outbursts of noise that lead to switching between the states. The typical time between such outbursts is much larger than t_r , whereas the duration of the switching event itself is comparable to t_r . Therefore the switching events are expected to be uncorrelated and described by the Poissonian statistics.

In order to detect interstate switching events when the switching rate is much smaller than the relaxation rate, one would need to set a threshold. Such threshold is related to but does not coincide with the basin boundary of the two stable states. Obtaining it requires separating the trajectories of random motion in which the system moves comparatively far in phase space from the initially occupied state but quickly comes back to it. For example, for a particle in a double-well potential, a trajectory that reaches the barrier top does not necessarily leads to switching. Here, even in the simplest case of fluctuations induced by white noise, to find the switching rate one has to set up a threshold sufficiently far beyond the barrier top with respect to the initially occupied state, as has been known since the classical work of Kramers [25]. It is clear from the above arguments that the thresholds for transitions between different states should not coincide, cf. [26].

Interstate switching can be well characterized by studying the vibration amplitude R . Respectively, we introduce two thresholds, R_{t_L} and R_{t_H} for $R(t)$, see Fig. 2 a. If the system was fluctuating about the $R = 0$ state and its trajectory $R(t)$ crossed R_{t_H} , we assume that it has switched to the large-amplitude state. On the other hand, if the system was fluctuating about the large-amplitude state and its trajectory $R(t)$ crossed R_{t_L} , we assume that it has switched to the $R = 0$ -state. It is critically important that the results do not depend on the precise values of R_{t_L} and R_{t_H} . The boundary that separates the basins of attraction to the stable states lies well between these values.

With the above definition, we further introduce the dwell (residence) times τ_{up} and τ_{down} . These are the

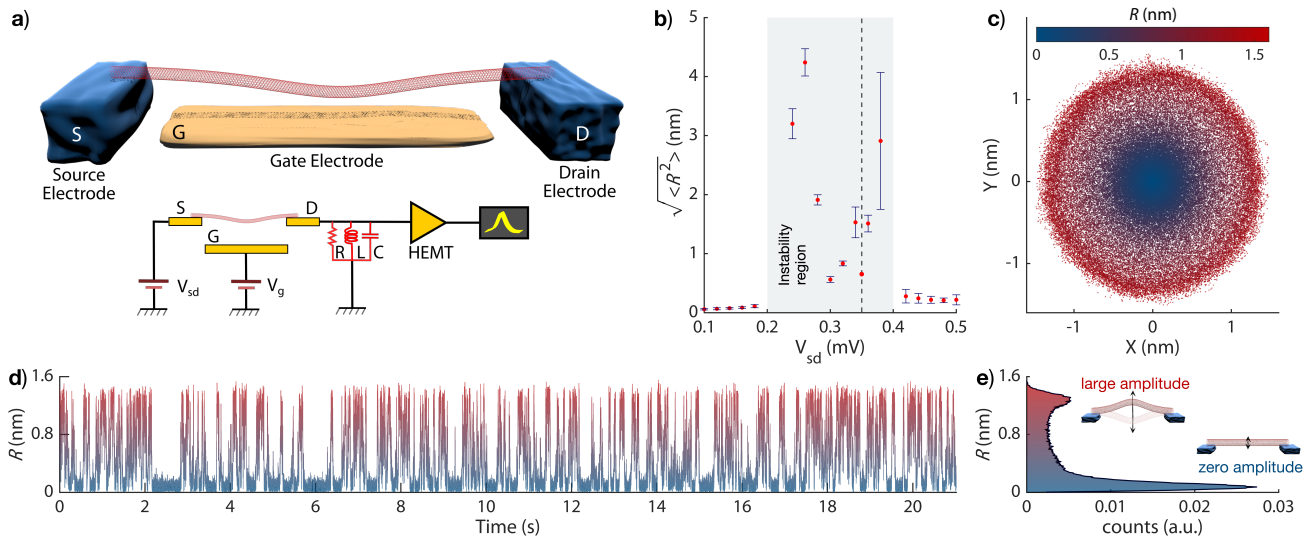


Fig. 1: Self-sustained oscillations and intermittent dynamics of the nanotube as a function of V_{sd} . **a**, Nanotube electromechanical oscillator and measurement schematic. Voltages V_{sd} and V_g are applied to electrodes S and G, respectively. Electrode D is connected to an RLC resonator. **b**, The standard deviation of the nanotube displacement $\sqrt{\langle R^2 \rangle}$ as a function of the source-drain voltage V_{sd} for gate voltage $V_g = -616$ mV (Fig. 3 c of [19]). $\sqrt{\langle R^2 \rangle}$ is obtained from spectral noise measurements for all the data points except for $V_{sd} = 0.35$ mV (dashed line); the latter is obtained by recording the time evolution of the displacement amplitude. At this voltage, the oscillations of the nanotube are characterized by means of **c**, the phase space of the two quadratures of the motion (X,Y) **d**, fluctuations of the amplitude $R = \sqrt{X^2 + Y^2}$ in time and **e**, the amplitude histogram, normalized with respect the total number of observations.

times spent in the zero- and large-amplitude states, respectively, before the system switches from these states.

Figures 2 b and 2 c show time evolution of the nanotube amplitude and the pattern of the trajectories on the quadrature plane (the X – Y plane). The time intervals τ_{up} and τ_{down} spent by the vibrational mode as it fluctuates about the large- and zero-amplitude states are shown in Fig 2 b by the red and blue thick bars, respectively. These intervals refer to the chosen boundaries R_{t_H} and R_{t_L} . The region between these boundaries on the phase plane contains the separatrix which separates the basins of attraction of the stable states. The experimental data do not allow us to find the separatrix. The motion of the oscillator in the rotating frame is slowed down near the separatrix for very small noise intensity, but in the experiment the noise is not that small and the time spent between R_{t_H} and R_{t_L} is $\sim t_r$.

Figures 2 d and 2 e show the distribution of the dwell times τ_{up} and τ_{down} . The transitions between states are well described by a Poisson process, and the distribution of the dwell times is close to exponential,

$$P(\tau) = \frac{1}{\langle \tau \rangle} e^{-\tau/\langle \tau \rangle}. \quad (1)$$

We use Eq. (1) to fit the experimental data. The dwell times τ_{down} and τ_{up} are given by the values of $\langle \tau \rangle$ for the corresponding transitions. From the fits, we find that these values are approximately the same for the chosen V_{sd} , with $\tau_{up} \approx \tau_{down} \approx 21$ ms. These values are much larger than the relaxation time ($t_r = 1-3$ ms) of the nan-

otube, which can be inferred from duration of the switching events themselves: in Fig. 2 b the trajectories leading to transitions are essentially vertical. The transition duration may not be estimated on the scale of the Fig. 2 b. The detailed data indicates that this duration is on the order of 1-3 ms (τ_s in Fig. 2 g). We also note that the fit of the exponential distribution of dwell times in Fig. 2 d,e is only mildly influenced by the bin size (see Fig. 2 f).

We repeated this statistical analysis for various combinations of thresholds to ensure the reliability and stability of the two-threshold approach. In Fig. 2 g we show the result of this analysis. We plot the extracted dwell times over a broad range of mean threshold values $(R_{t_H} + R_{t_L})/2 \in [0.7, 0.9]$ nm and the separations $R_{t_H} - R_{t_L} \in [0.2, 0.4]$ nm. The results do not change, essentially. This is a direct indication of the system performing noise-induced hopping between its two metastable states.

To further confirm the interpretation of the dynamics of the system as resulting from switching between the metastable state at $R = 0$ and the metastable state of self-sustained vibrations, we conducted our stochastic analysis for temporal data that refer to $V_{sd} = 0.25$ mV and $V_g = -616$ mV, see Supplementary Information. Section I [27]. The dwell times are different for these parameters, but the overall picture holds.

Nonlinear friction force and self-oscillations. We now discuss the potential origin of the bistable dynamics observed in Fig. 2. The variation of conductance of the CNT with voltage was previously reported in [19] and

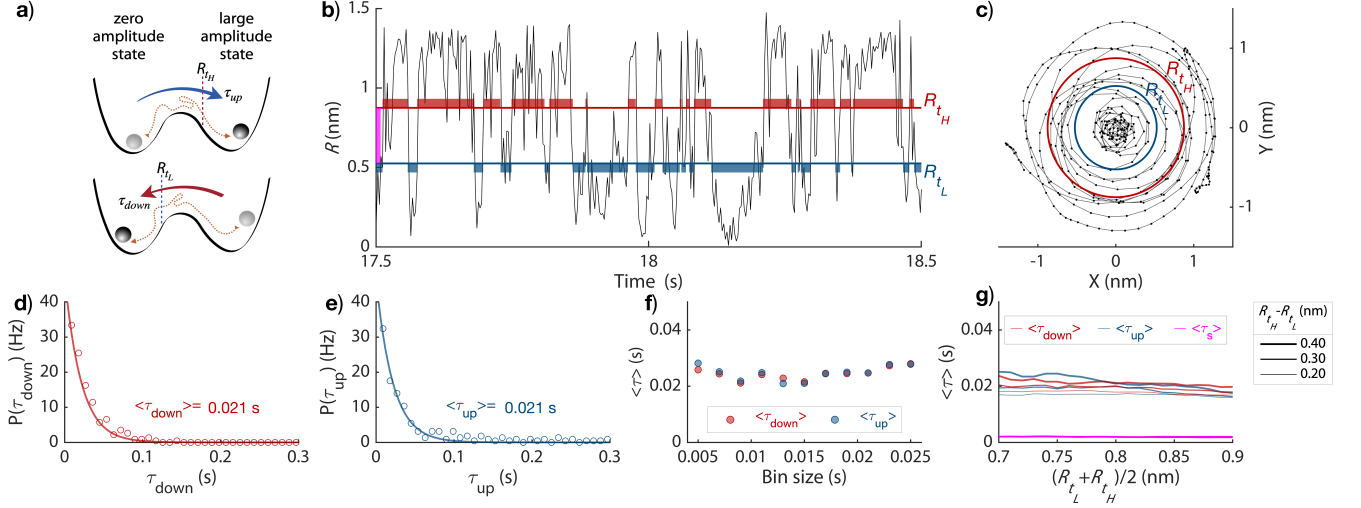


Fig. 2: Motion statistics of the carbon nanotube at $V_{sd} = 0.35$ mV and $V_g = -616$ mV. **a**, Schematic energy surface of the system with two stable states. The CNT transitions form the zero/large to the large/zero amplitude state after a time τ_{up}/τ_{down} by crossing the threshold R_{tH}/R_{tL} . **b**, Time evolution of the motion amplitude. Blue/red bars digitize the residence time among the zero/large amplitude state. **c**, Evolution of the trajectory in the phase space of the two quadratures between 17.65 and 17.7 s. The system crosses the threshold lines R_{tL} and R_{tH} multiple times filling the X-Y space ($R_{tH} - R_{tL} = 0.35$ nm, $(R_{tH} + R_{tL})/2 = 0.7$ nm). **d-e**, Dwell (residence) time distributions (bin size 9 ms) from the large to the zero amplitude state (panel d) and from the zero to the large (panel e). A Poissonian process with Eq. (1) is fitted to the data and gives averaged dwell times of $\langle \tau_{down} \rangle = 0.021$ s and $\langle \tau_{up} \rangle = 0.021$ s. **f**, Influence of the bin size on the average dwell times in panels d and e. **g**, Average dwell times for varying thresholds R_{tL} and R_{tH} . The average time $\langle \tau_s \rangle$ is the time spent in between the two thresholds, within which the separatrix is located. (vertical magenta bar in panel b).

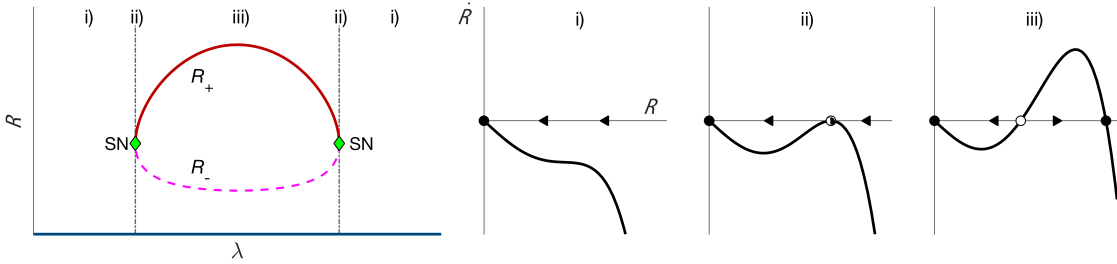


Fig. 3: Emergence of isola bifurcation as a result of non-monotonic nonlinear damping. Steady-state solutions as a function of the bifurcation parameter λ . Solid/dashed lines are stable (R_+)/unstable (R_-) solution branches. Panel i) is the radial phase portrait below and above the SN point. The solid dot is a stable solution (attracting state). ii) Saddle-node bifurcation of cycle (SN) with the half-stable solution (half-filled circle). iii) Bistable region with co-existing zero and large amplitude states. The open circle is a unstable repelling solution. The arrows in panels i), ii), iii) indicates the dynamical flow.

shows a complicated pattern in the regime of bistability. It can be related not just to the interplay of the nanotube vibrations and the charge on the nanotube, but also to Joule heating, the properties of the contacts and the delay in the external circuit. This complicates development of a microscopic theory of the nanotube dynamics. Instead, here we propose a minimalistic phenomenological theory that leads to the observed behavior.

A major observation to explain is the “hard” excitation and collapse of self-sustained vibrations with the varying drive V_{sd} , where the vibrations emerge and collapse while their amplitude remains finite and the system remains bistable. Such behavior can be associated with the change of the nonlinear friction force. The nonlin-

ear friction force is well-known in nanomechanics, see [1]. Usually it leads to a faster decay of vibrations with the increasing amplitude, that is, the coefficient of nonlinear friction is positive, although in periodically modulated one- [28] and two-mode [22] systems this coefficient can become negative in a certain range of the modulation parameters.

Since the vibration frequency is much higher than all other rates and frequencies in the system, the vibrations can be described in the rotating frame using a complex vibration amplitude $z(t) = C_z [q + i(p/m\omega_0)] \exp(i\omega_0 t)$, where q and p are the mode coordinate and momentum, m is its effective mass, and ω_0 is the eigenfrequency (see Supplementary Information Section II [27]; C_z is the scal-

ing parameter). In the equation of motion of $z(t)$ one has to take into account the linear and nonlinear friction as well as the Duffing nonlinearity of the mode. In the rotating wave approximation this equation reads

$$\dot{z} = - [\Gamma + (\gamma_{\text{nlf}} - i\gamma_D)|z|^2 + |z|^4] z. \quad (2)$$

Here Γ and γ_{nlf} are the standard coefficients of linear and nonlinear friction, whereas γ_D is the Duffing nonlinearity. We note that the structure of the equation is fully dictated by the rotating-wave approximation, which applies, in particular, provided $|\dot{z}| \ll \omega_0|z|$. The right-hand side is essentially an expansion in z , which applies provided the vibration amplitude is comparatively small, so that the decay rate and the change of the vibration frequency are $\ll \omega_0$. The absence of delay in Eq. (2) is justified if the delay is small compared to the ‘‘slow’’ time of order Γ^{-1} , whereas it may be significant on a short time scale, for example, on the time scale ω_0^{-1} .

In contrast to the frequently used model of the single-mode dynamics we have incorporated into the right-hand side of Eq. (2) the term $\propto |z|^4 z$. This term describes a higher-order nonlinear friction and must be taken into account where the conventional friction coefficients Γ and γ_{nlf} become small. A simple classical microscopic model of such friction is described in the Supplementary Information III. In quantum terms, the friction comes from processes in which the considered mode makes a transition over three quantum energy levels with emission of energy $\approx 3\hbar\omega_0$ into the thermal reservoir.

We can rewrite Eq. (2) in polar coordinates by setting $z(t) = R(t)e^{i\theta(t)}$, where R and θ are the vibration amplitude and the ‘‘slow’’ part of the vibration phase. From Eq. (2)

$$\dot{R} = -f_{\text{nlf}}R, \quad \dot{\theta} = \gamma_D R^2, \quad (3)$$

where the nonlinear friction force is

$$f_{\text{nlf}} = \Gamma + \gamma_{\text{nlf}}R^2 + R^4. \quad (4)$$

Equations (3) and (4) without the term R^4 in f_{nlf} have been broadly used in the literature, from electronics, to lasers as well as nano- and micro-mechanics to describe the onset of self-oscillations. In the conventional analysis it is assumed that the parameter γ_{nlf} is positive. In this case the quiet state $R = 0$ is stable for the linear friction coefficient $\Gamma > 0$. Once Γ becomes negative, the state $R = 0$ becomes unstable and there emerges a stable limit cycle on the plane $(R \cos \theta, R \sin \theta)$ with radius $(|\Gamma/\gamma_{\text{nlf}}|)^{1/2}$, which is given by equation $f_{\text{nlf}} = 0$. It corresponds to vibrations in the laboratory frame with amplitude $\propto (|\Gamma/\gamma_{\text{nlf}}|)^{1/2}$. The corresponding bifurcation is called supercritical Hopf bifurcation.

On the other hand, if Γ is positive, the state $R = 0$ is stable. Once the condition $\gamma_{\text{nlf}} < 0$ is met, there emerges an unstable limit cycle with a radius $(\Gamma/|\gamma_{\text{nlf}}|)^{1/2}$ (a subcritical Hopf bifurcation). If R exceeds $(\Gamma/|\gamma_{\text{nlf}}|)^{1/2}$, it increases in time by moving away from this cycle.

The term R^4 in f_{nlf} can significantly modify the dynamics for $\gamma_{\text{nlf}} < 0$ and $\Gamma > 0$. It is seen from Eq. (3) that, along with the unstable limit cycle, there emerges a stable limit cycle. The radii of the cycles as given by the condition $f_{\text{nlf}} = 0$ are

$$R_{\pm} = \frac{1}{\sqrt{2}} \left[-\gamma_{\text{nlf}} \pm \sqrt{\gamma_{\text{nlf}}^2 - 4\Gamma} \right]^{1/2} \quad (5)$$

For $-\gamma_{\text{nlf}} > 2\Gamma^{1/2}$ the cycle with the radius R_+ is stable, whereas the cycle with the radius R_- is unstable. At $\gamma_{\text{nlf}} = -2\Gamma^{1/2}$ the two cycles merge and annihilate one another in a saddle-node bifurcation. For smaller $|\gamma_{\text{nlf}}|/2\Gamma^{1/2}$ they disappear.

The isola bifurcation. We now relate the generic model (2) to the experiment keeping in mind that Γ and γ_{nlf} change with a bifurcation parameter λ , which, based on Fig. 1 b, is associated with the variation in the nanotube drive, i.e. $\lambda = \lambda(V_{\text{sd}})$. The key experimental observations can be summarized as follows: (i) a stable zero-amplitude state and a stable large-amplitude state (limit cycle) coexist in a certain parameter range, (ii) the zero-amplitude state is stable outside this range, and (iii) the limit cycle is excited and collapses with the varying parameters while having a large amplitude.

The stability of the $R = 0$ -state means that $\Gamma > 0$, that is, the linear damping does not change sign. This naturally excludes the scenario in which a supercritical Hopf bifurcation leads to limit cycle oscillations and the $R = 0$ state becomes unstable. In contrast, in the model (2) a stable limit cycle and a stable zero-amplitude state coexist in the parameter range $\gamma_{\text{nlf}} < 0$ and $-\gamma_{\text{nlf}} > 2\Gamma^{1/2}$. Then a minimalistic picture that describes the experiment is that, as the source-drain voltage V_{sd} varies, there first occurs a saddle-node bifurcation where there emerge the stable and unstable limit cycle with amplitudes R_{\pm} , but then these limit cycles again merge together and disappear in the saddle-node bifurcation. This picture also applies if the dynamics is more complicated than what Eq. (2) suggests.

In the above minimalistic picture, the values of R_+ and R_- as functions of V_{sd} form a loop, cf. Fig. 3. The values of V_{sd} where the loop emerges and disappears are isola bifurcations [21]. One part of the loop corresponds to a stable limit cycle (with radius R_+), whereas the other part corresponds to the unstable limit cycle. They merge for the values of V_{sd} where, in the model (3), $\gamma_{\text{nlf}} = -2\Gamma^{1/2}$.

To relate the above minimalistic model to Eqs. (3) and (4) we should consider how the parameters of these equations depend on V_{sd} . A major factor is the V_{sd} -dependence of γ_{nlf} , since this parameter becomes negative and, moreover, exceeds $2\Gamma^{1/2}$ in the absolute value. It should be noted that the linear friction coefficient Γ also depends on V_{sd} , as reported in [19]. Overall, these dependences should be nonmonotonic to allow for both the onset and the disappearance of the bistability with the increasing V_{sd} .

The analysis simplifies if the range of V_{sd} in which the zero-amplitude state coexists with the vibrational state is narrow. In this case one can approximate

$$\gamma_{\text{nlf}}(V_{sd}) + 2\sqrt{\Gamma(V_{sd})} = -\eta(V_B^{(1)} - V_{sd})(V_{sd} - V_B^{(2)}) \quad (6)$$

Here $V_B^{(1,2)}$ are the bifurcational values of the voltage V_{sd} . The system shows bistability in the range where $V_B^{(2)} < V_{sd} < V_B^{(1)}$. Here, the parameter $\eta > 0$ is a scaling parameter.

Beyond a narrow range near the isola bifurcation point, the dependence of the friction parameters on V_{sd} is more complicated than Eq. (6) and is generally nonmonotonic. The microscopic mechanism of this dependence is beyond the scope of the present paper. The overall coupled dynamics of the electron and vibrational systems is complicated, in part because of the disorder at the contact area of the nanotube and nonuniformity of the nanotube itself. We would mention that the interplay of the Joule heating and retardation in the circuit (delayed feedback) leads to the decrease of the linear friction coefficient Γ [19]. Delayed feedback may also transform the nonlinear dependence of the nanotube conductance on the vibration amplitude into a negative nonlinear friction.

It is important that, because of the small positive linear damping and small intrinsic nonlinear friction of the CNT, which are observed in the limit of small V_{sd} , already a small delayed feedback can be sufficient to result in the observed instability for larger V_{sd} . We note that the Markovian approximation of the “instantaneous” linear and nonlinear friction, which we are using, holds in the rotating frame on the time scale much longer than the vibration period.

To conclude, we demonstrate that the analysis of the stochastic dynamics of a nanomechanical system allows revealing novel phenomena that may remain undetected in the absence of noise. Specifically, we show that driv-

ing a carbon nanotube by a dc source-drain voltage V_{sd} leads to the onset of a non-hysteretic bistability, in which a stable quiet state coexists with a stable state of periodic self-sustained vibrations. Varying V_{sd} in the absence of noise would not lead to the onset of the vibrations. The vibrations are excited, and thus become manifested, due to fluctuations. The bistability is characterized by studying noise-induced switching between the coexisting stable states and demonstrating that the switching displays the Poisson statistics typical of uncorrelated random events.

We further show that the vibrational state exists in an isolated region of the parameter space and emerges as a result of an isola bifurcation. The occurrence of an isola was documented in the past for two nonlinearly coupled periodically driven microscale vibrational modes [22]. However, to the best of our knowledge an isola has not been seen in a single-mode system in the absence of periodic driving.

We provide a minimalistic phenomenological model of the isola bifurcation associated with the occurrence of bistability in a nanomechanical system and provide the normal form of the bifurcation. The bistability results from two saddle-node bifurcations in which the same branches of a stable and an unstable vibrational state emerge/disappear. In the phase space these branches form a loop. The phenomenon is related to the nonlinear friction coefficient becoming negative in the corresponding parameter range.

Our stochastically-unveiled bistable dynamics expands on the new intriguing phenomena recently found in CNTs, such as the cooling of vibrations down to a few quanta [19], the ultrastrong coupling regime [29], mechanical nonlinearities for vibrations approaching the quantum ground state [30], and the enhancement of the coupling between vibrations and radio-frequency photons via the quantum capacitance [31]. Our results demonstrate qualitatively new aspects of the interplay of fluctuations and nonlinear dynamics in vibrational systems.

-
- [1] A. Bachtold, J. Moser, and M. I. Dykman, *Rev. Mod. Phys.* **94**, 045005 (2022).
- [2] D. S. Greywall, B. Yurke, P. A. Busch, A. N. Pargellis, and R. L. Willett, *Phys. Rev. Lett.* **72**, 2992 (1994).
- [3] L. G. Villanueva, E. Kenig, R. B. Karabalin, M. H. Matheny, R. Lifshitz, M. C. Cross, and M. L. Roukes, *Phys. Rev. Lett.* **110**, 177208 (2013).
- [4] E. Kenig, M. C. Cross, J. Moehlis, and K. Wiesenfeld, *Phys. Rev. E* **88**, 062922 (2013).
- [5] C. Stambaugh and H. B. Chan, *Phys. Rev. Lett.* **97**, 110602 (2006).
- [6] J. S. Huber, G. Rastelli, M. J. Seitner, J. Kölbl, W. Belzig, M. I. Dykman, and E. M. Weig, *Phys. Rev. X* **10**, 021066 (2020).
- [7] E. Buks and B. Yurke, *Phys. Rev. A* **73**, 023815 (2006).
- [8] F. Yang, M. Fu, B. Bosnjak, R. H. Blick, Y. Jiang, and E. Scheer, *Phys. Rev. Lett.* **127**, 184301 (2021).
- [9] M. Dykman and M. Krivoglaz, *Physica A: Statistical Mechanics and its Applications* **104**, 480 (1980).
- [10] M. I. Dykman, *Phys. Rev. E* **75**, 011101 (2007).
- [11] J. S. Aldridge and A. N. Cleland, *Phys. Rev. Lett.* **94**, 156403 (2005).
- [12] H. B. Chan and C. Stambaugh, *Phys. Rev. Lett.* **99**, 060601 (2007).
- [13] R. B. Karabalin, R. Lifshitz, M. C. Cross, M. H. Matheny, S. C. Masmanidis, and M. L. Roukes, *Phys. Rev. Lett.* **106**, 094102 (2011).
- [14] W. J. Venstra, H. J. R. Westra, and H. S. J. van der Zant, *Nat. Commun.* **4**, 2624 (2013).
- [15] M. Defoort, V. Puller, O. Bourgeois, F. Pistolesi, and E. Collin, *Phys. Rev. E* **92**, 050903 (2015).
- [16] A. Chowdhury, S. Barbay, M. G. Clerc, I. Robert-Philip, and R. Braive, *Phys. Rev. Lett.* **119**, 234101 (2017).
- [17] R. J. Dolleman, P. Belardinelli, S. Houri, H. S. J. van der Zant, F. Aljani, and P. G. Steeneken, *Nano Lett.* **19**, 1282 (2019).

- [18] O. Usmani, Y. M. Blanter, and Y. V. Nazarov, *Phys. Rev. B* **75**, 195312 (2007).
- [19] C. Urgell, W. Yang, S. L. De Bonis, C. Samanta, M. J. Esplandiú, Q. Dong, Y. Jin, and A. Bachtold, *Nat. Phys.* **16**, 32 (2020).
- [20] Y. Wen, N. Ares, F. J. Schupp, T. Pei, G. A. D. Briggs, and E. A. Laird, *Nat. Phys.* **16**, 75 (2020).
- [21] D. Dellwo, H. B. Keller, B. J. Matkowsky, and E. L. Reiss, *SIAM J. Appl. Math.* **42**, 956 (1982), 2101093.
- [22] X. Dong, M. I. Dykman, and H. B. Chan, *Nature Communications* **9**, 3241 (2018).
- [23] J. Moser, A. Eichler, J. Guetinger, M. I. Dykman, and A. Bachtold, *Nat. Nanotech* **9**, 1007 (2014).
- [24] A. Zakharova, T. Vadivasova, V. Anishchenko, A. Koseska, and J. Kurths, *Phys. Rev. E* **81**, 011106 (2010).
- [25] H. Kramers, *Physica* **7**, 284 (1940).
- [26] M. I. Dykman, G. P. Golubev, D. G. Luchinsky, A. L. Velikovich, and S. V. Tsuprikov, *Phys. Rev. A* **44**, 2439 (1991).
- [27] Supplementary information.
- [28] M. I. Dykman, G. Rastelli, M. L. Roukes, and E. M. Weig, *Phys. Rev. Lett.* **122**, 254301 (2019).
- [29] F. Vigneau, J. Monsel, J. Tabanera, K. Aggarwal, L. Bresque, F. Fedele, F. Cerisola, G. A. D. Briggs, J. Anders, J. M. R. Parrondo, A. Auffèves, and N. Ares, *Phys. Rev. Res.* **4**, 043168 (2022).
- [30] C. Samanta, S. L. De Bonis, C. B. Møller, R. Tormo-Queralt, W. Yang, C. Urgell, B. Stamenic, B. Thibeault, Y. Jin, D. A. Czaplewski, F. Pistolesi, and A. Bachtold, *Nature Physics* **19**, 1340 (2023).
- [31] S. Blien, P. Steger, N. Hüttner, R. Graaf, and A. K. Hüttel, *Nat Commun* **11**, 1636 (2020).

Acknowledgments

Financial support was provided from the European Union’s Horizon 2020 research and innovation programme under ERC starting grant no. 802093 and ERC advanced grant no. 692876. MD acknowledges partial support by the Moore Foundation grant no. 12214. AB acknowledges MICINN Grant No. RTI2018-097953-B-I00 and PID2021-122813OB-I00, AGAUR (Grant No. 2017SGR1664), the Fondo Europeo de Desarrollo, the Spanish Ministry of Economy and Competitiveness through Quantum CCAA, TED2021-129654B-I00, EUR2022-134050, and CEX2019-000910-S [MCIN/AEI/10.13039/501100011033], MCIN with funding from European Union NextGenerationEU(PRTR-C17.I1) and Generalitat de Catalunya, CERCA, Fundacio Cellex, Fundacio Mir-Puig.

Data availability

Data supporting the findings in this manuscript are available upon request.

Competing interests

We declare we have no competing interests.